Reduced Complexity Satellite Broadcast Receiver with Interference Mitigation in Correlated Noise

Zohair Abu-Shaban, *Student Member, IEEE*, Hani Mehrpouyan, *Member, IEEE*, Bhavani Shankar M. R, *Senior Member, IEEE*, and Björn Ottersten, *Fellow, IEEE.*

***Abstract*—The recent commercial trends towards using smaller dish antennas for satellite receivers, and the growing density of broadcasting satellites, necessitate the application of robust adjacent satellite interference cancellation schemes. This orbital density growth along with the wider beamwidth of a smaller dish have imposed an *overloaded* scenario at the satellite receiver, where the number of transmitting satellites exceeds the number of receiving elements at the dish antenna. To ensure successful operation in this practical scenario, we propose a satellite receiver that enhances signal detection from the desired satellite by mitigating the interference from neighboring satellites. Towards this objective, we propose an enhanced list-based group-wise search detection (E-LGSD) receiver under the assumption of spatially correlated additive noise. To further enhance detection performance, the proposed satellite receiver utilizes a newly designed whitening filter to remove the spatial correlation amongst the noise parameters, while also applying a preprocessor that maximizes the signal-to-interference-plus-noise ratio. We exploit the structure of this filter and propose a reduced complexity LGSD (RC-LGSD) receiver. Extensive simulations under practical scenarios show that the proposed receiver enhances the performance of satellite broadcast systems in the presence of ASI compared to existing methods. Also, under pointing error, RC-LGSD exhibits similar behavior to that of the optimum receiver.**

I. Introduction

Over the past decade, satellite broadcast services including, direct-to-home (DTH), have shown steady growth that is expected to continue in the future [1]. To meet the needs of satellite broadcast market, more satellites are launched and typically stationed in the geostationary orbit (GEO), resulting it higher satellite density and making receivers more susceptible to *adjacent satellite interference* (ASI) [2]. Although satellite receivers with small-aperture antennas are more commercially attractive, they possess a wider radiation pattern resulting in a reduced directivity and higher ASI. These factors make it a priority to design new algorithms that can effectively mitigate the ASI. Such algorithms are expected to enhance the throughput of satellite receivers and provide the satellite broadcasting industry with an edge over other existing alternatives, e.g., cable and fiber optics.

To combat ASI, receivers with multiple-feed antenna, known as *multiple low noise blocks* (MLNBs) have been used to beamform towards the desired satellite, whose location is known [3]–[5]. The high number of satellites fall within the view of wide patterns of small dish antennas relative to the limited MLNBs, typically $2-3$, gives a rise to an overloaded scenario. Fig. 1 illustrates a conceptual setup of this principle.

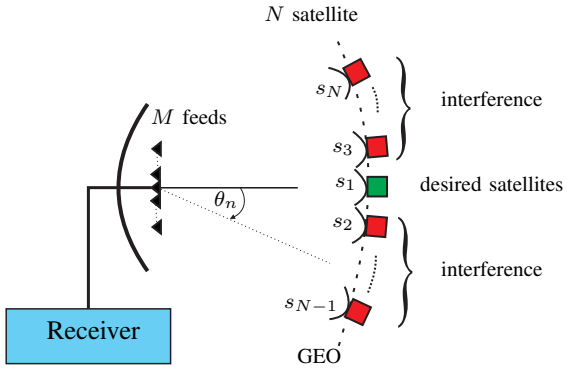

Fig. 1. The system setup for N satellites in the geostationary orbit, and $M < N$ LNBs. The dish is directed to the desired satellite, s_1.

ASI cancellation for signals with partial frequency overlap is addressed in [6] and [7], with the latter particularly addressing signals conforming to the digital video broadcasting standard, DVB-S2 [8]. However, [6] and [7] employ a single input receiver, and do not exploit spatial processing. On the other hand, an MLNB-based two-stage satellite receiver is proposed in [4]. It applies a linear preprocessing that minimizes the overloading effect on the non-linear iterative detection in the following stage. However, this receiver exhibits a poor bit error rate (BER) performance for QPSK signals, which is expected to worsen for the higher order modulations, considered herein.

ASI mitigation for *full* frequency overlap satellite systems is addressed in [5]. While considering the satellite position relative to the antenna orientation, [5] applies a successive interference cancellation (SIC) along with two different beamforming methods to mitigate the impact of ASI. The aim of [5] is to detect the signals from as many satellites as the number of the LNBs that are available at the receiver. Although the algorithm shows an acceptable bit-error rate performance for QPSK satellite signals, the performance greatly deteriorates as the modulation order increases.

For non-satellite scenarios, co-channel interference cancellation techniques for *overloaded* receivers are discussed in [9]–[14]. These works are generally based on the maximum-likelihood approach or a lower complexity variation of it. Although the joint maximum-likelihood (JML) detector is optimal [9], its complexity grows exponentially with the number of transmitted signals and the modulation order, making its application in modulations schemes used in DVB-S2, e.g., 8PSK 16APSK, prohibitively unfeasible.

Zohair Abu-Shaban is with the Research School of Engineering at the Australian National University, Canberra, Bhavani Shankar R and Björn Ottersten are with the Interdisciplinary Centre for Security, Reliability and Trust at the University of Luxembourg, Luxembourg. Hani Mehrpouyan is with the Department of Electrical and Computer Engineering at Boise State University, Idaho. Emails: zohair.abushaban@anu.edu.au, hani.mehr@ieee.org, bhavani.shankar@uni.lu, bjorn.ottersten@uni.lu.

This work is partly supported by the National Research Fund (FNR), Luxembourg. Project ID: 4043055, and the NASA Young Investigator Seed grant.

A two-stage receiver with a search-based algorithm known as *list-based group search detection* (LGSD) is proposed in [10]. LGSD searches over a smaller space compared to the JML detector by estimating a list of highly probable candidates. As *linear preprocessing*, the first stage uses maximum ratio combining (MRC) to maximize the received signal-to-noise ratio (SNR). Subsequently, the receiver employs a non-linear detector that comprises two processes. The first process creates a shortlist of candidates and forwards it to the second process to execute JML detection. In essence, LGSD partitions the channel matrix into lower dimensional search spaces, before executing JML detection on the related sub-vector of the received signal. Iterating between the two processes can improve the performance with some added complexity. Although LGSD reduces the complexity of JML detection in overloaded scenarios, it is not directly applicable to satellite broadcast receivers, because the interference is modelled by a white Gaussian random process, and the additive receiver noise is assumed to be uncorrelated. These two assumptions may not hold for satellite broadcast systems [3]–[5].

In this paper, we design an overloaded multiple-input receiver for satellite broadcast systems, which uses a small-size antenna with a radius less than 40 cm, equipped with MLNBs. As shown in Fig. 1, the dish is assumed to be fixed and directed towards the central satellite, which we refer to as the *desired* satellite. The remaining satellites in the view of the antenna are also assumed to be operating in the same frequency band and are referred to as the *interfering* satellites. Due to the small dish size, the antenna patterns are wide, causing a high level of interference. We propose the *enhanced-LGSD* (E-LGSD) receiver that improves the conventional LGSD method and address its shortcomings by changing the interference and noise model to ones more appropriate in satellite broadcast systems. We further introduce a channel truncation in the second stage to reduce the computational complexity of the E-LGSD, and refer to this receiver as the *reduced-complexity* LGSD (RC-LGSD). Our contributions can be summarized as:

- We accurately model the ASI of the neighboring satellites assuming known satellite locations and fixed antenna setup. This enable us to apply a beamformer based on signal-to-interference-plus-noise (SINR) maximization criterion.
- We use an additive noise model that accounts for the spatial correlation amongst the MLNBs, resulting from the overlapping radiation patterns [4], and derive a new whitening filter that is appropriate for the new noise model and proposed beamformer. We propose the E-LGSD based on the new noise and interference models.
- The linear preprocessor of E-LGSD computes an equivalent channel matrix. However, because the system considered herein is overloaded, this matrix have rows of zeros, making it rank deficient. Thus, we truncate the channel matrix to reduce the number of calculations, and effectively the complexity, required to create the candidate list for LGSD. Based on this truncation, we improve the performance of the E-LGSD, and propose RC-LGSD receiver.
- We carry out extensive Monte-Carlo simulations to investigate the performance of the proposed receiver in realistic scenarios. Our simulations show that RC-LGSD can outperform the conventional LGSD [10], while having less complex than E-LGSD [15]. Moreover, we perform an in-depth numerical investigation on the impact of various algorithm parameters and the interesting trade-off between performance and complexity. Finally, we evaluate the receiver performance in the presence of pointing errors.

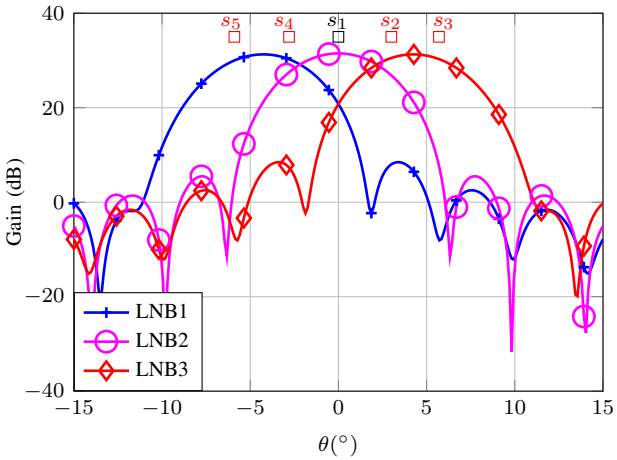

Fig. 2. Radiation patterns of three LNBs mounted on a 35-cm dish.

Preliminary results of this work were presented in [15].

The rest of the paper is organized as follows: Section II highlights the system model and the underlying assumptions. Section III describes the proposed receivers, highlighting the proposed preprocessor, beamformer and noise whitening filter. The complexities of the proposed and existing algorithms are analyzed in Section IV. The numerical results are discussed in Section V, while Section VI concludes the paper.

II. Assumptions and Signal Model

In the light of Fig. 1, consider N adjacent satellites orbiting the GEO and broadcasting to a receiver equipped with a small-size dish and M LNBs. We make the following assumptions:

- *Overloaded receiver ($N > M$)*: Due to practical factors such as cost reduction and electromagnetic blockage prevention, M is small, typically 2–3. On the other hand, for small-aperture reflectors, the beamwidth is large, causing N to be large. Depending on the dish diameter, D, and the wavelength λ, the reflector's 3-dB beamwidth can be estimated by $(70\lambda/D)^\circ$ [16]. Based on that, N can then be estimated knowing that GEO satellites are separated by an angular spacing[1] of $2.5^\circ - 3^\circ$ [4]. Although having more LNBs extends the field-of-view, allowing more interference into the system, it offers additional degrees of freedom and enables beamforming, and enhances the joint detection. Fig. 2 shows the antenna patterns for 35-cm dish equipped with 3 LNBs. It can be seen that 3 satellites fall within the view of the central LNB, while in total, 5 satellites are seen by the 3 LNBs.

[1]For example, a single-LNB dish with 35 cm diameter, operating in the Ku-band, has a 3-dB beamwidth of $5^\circ - 6^\circ$. Thus, the field-of-view contains $2 - 3$ satellites.

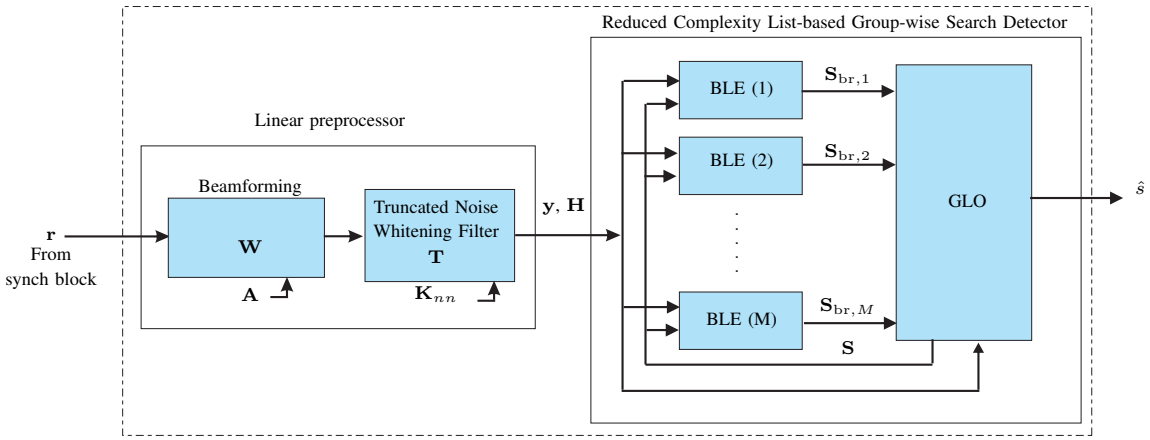

Fig. 3. The block diagram of the proposed receiver. BLE: Branch list estimator. GLO: Global list optimizer.

- *The system is synchronized:* Although the LNBs can use the same oscillator to reduce the frequency and phase uncertainties, the received signals are assumed to be symbol-synchronized via a synchronization block at the digital front-end of the receiver. Such an assumption has been made in prior works e.g., [3]–[5].
- *Spatially correlated noise:* Similar to [3]–[5], the radiation patterns of the LNBs are assumed to partially overlap. This induces spatial correlation in the noise emanating from other sources such as uplink noise and satellite components.
- *The signals are compliant with DVB-S2 and are transmitted independently:* Signal parameters such as modulation and power level can be estimated by the receiver using the frame structure defined in DVB-S2. Since these parameters are already needed for synchronization, we assume that they are provided by the synchronization block. Such an assumption has been also made in prior work in [3].
- *The channel is static and known:* We assume a line-of-sight path and a clear sky. Therefore, the channel is mainly dependent on parameters such as the antenna geometry and specifications. Since these parameters do not vary quickly, they are assumed fixed over the transmission interval. Accordingly, the channel is expressed as a function of the satellite orbital angles, which can be estimated by the knowledge of the antenna radiation patterns. Although ideal channel is assumed, we introduce pointing errors, and evaluate the performance under pointing angle uncertainty.

Under these assumptions, the baseband symbol-sampled received signal at the output of the synchronizer is given by

$$\mathbf{r}[k] = \mathbf{A}\mathbf{s}[k] + \mathbf{n}[k], \tag{1}$$

where $\mathbf{r}[k] \in \mathbb{C}^M$ is the received symbol vector at time instant k, $\mathbf{A} \triangleq [A_{i,j}] \in \mathbb{C}^{M\times N}$ is the antenna response matrix with $A_{i,j}$ denoting the complex gain of the i^{th} LNB in the direction of the j^{th} satellite, $\mathbf{s}[k] \in \mathbb{C}^N$ is the transmitted symbol vector, such that the j^{th} element in $\mathbf{s}[k]$, $s_j[k]$, is drawn from a zero-mean unit-energy signal constellation Ω of cardinality K. For 8PSK and 16APSK, K =8 and 16, respectively. Without loss of generality, $s_1[k]$ corresponds to the desired satellite (Fig. 1).

Finally, $\mathbf{n}[k] \in \mathbb{C}^M$ is zero-mean additive Gaussian noise with covariance matrix $\mathbf{R}_{\text{nn}} = \sigma_n^2\mathbf{K}_{\text{nn}} \in \mathbb{C}^{M\times M}$. Here, σ_{n}^2 is the noise variance and $\mathbf{K}_{\text{nn}} \triangleq [K_{m,m'}]$ is the matrix of normalized correlation coefficients. Note that $\mathbf{K}_{\text{nn}}$ is a function of the radiation patterns of the LNBs and is determined by the magnitude of overlapping amongst these patterns. To obtain $K_{m,m'}$, denote the square root of the radiation pattern of the m^{th} LNB by $p_m(\theta)$, then [17]

$$K_{m,m'} = \frac{\int_{-\pi}^{\pi} p_m(\theta)p_{m'}^*(\theta)d\theta}{\sqrt{\int_{-\pi}^{\pi} p_m(\theta)p_m^*(\theta)d\theta}\sqrt{\int_{-\pi}^{\pi} p_{m'}(\theta)p_{m'}^*(\theta)d\theta}}, \tag{2}$$

where θ is in radians, and $(^*)$ is the complex conjugate operator. It is understood from (2) that when pattern overlapping is wider, the spatial correlation grows higher. This implies that for a small dish with a wide pattern, the additive noise at the outputs of the LNBs have stronger correlation.

Our objective is to detect the signal of the desired satellite $s_1[k]$, based on the received signal (1).

III. Proposed Overloaded Receiver Design

In this section, we discuss the design of the proposed overloaded satellite receiver. The block diagram of this two-stage receiver is illustrated in Fig. 3 and comprises:

1) A linear preprocessor stage, which is composed of a beamformer followed by a noise whitening filter. The objective of this stage is to reduce the overloading effect on the receiver performance by better optimizing the output with respect to the SINR criterion, while alleviating the impact of the correlated noise on the detection process.
2) The so-called RC-LGSD algorithm, which itself has two components. The first component is a bank of branch list estimators (BLE) that simultaneously nominate multiple candidate lists to be used in the second component of the algorithm, known as the global list optimizer (GLO). GLO uses these lists to determine the best ML estimate of the transmitted symbol vector. Finally, the output list of GLO is fed-back to the BLEs for further iterations.

A. Linear Preprocessor

Denoting the output of the linear preprocessor of the conventional LGSD by $\mathbf{r}'$, and dropping the time index k, $\mathbf{r}'$ can be written as

$$\mathbf{r}' = \mathbf{F}^H\mathbf{W}^H\mathbf{r} \triangleq \mathbf{A}'\mathbf{s} + \mathbf{n}', \tag{3}$$

where $\mathbf{W} \in \mathbb{C}^{M\times N}$ and $\mathbf{F} \in \mathbb{C}^{N\times N}$ are the beamforming and noise whitening filter matrices, respectively. $\mathbf{A}' \triangleq \mathbf{F}^H\mathbf{W}^H\mathbf{A}$ represents the equivalent channel matrix at the input of the detector and $\mathbf{n}' = \mathbf{F}^H\mathbf{W}^H\mathbf{n}$ is the whitened additive Gaussian noise process at the output of the preprocessor. In the following subsections, we design $\mathbf{W}$ and $\mathbf{F}$ for E-LGSD, before we truncate $\mathbf{F}$ to obtain $\mathbf{T}$ for RC-LGSD.

1) Beamforming: The conventional LGSD [10] uses an SNR-based (MRC) beamformer. However, in satellite systems the structure of the interference can be exploited to design an SINR-based beamformer that can further enhance the receiver performance. This is even more important since current satellite systems with small-size receiving dishes maybe more interference-limited than noise-limited. This conclusion is also supported by the simulation results presented in Section V. From [10], the MRC beamformer is defined as

$$\mathbf{W} = \mathbf{A}. \tag{4}$$

On the other hand, the n^{th} column of the beamforming matrix to maximize the SINR for the n^{th} stream is given by

$$\mathbf{w}_n \triangleq \arg\max_{\mathbf{w}\in\mathbb{C}^M} \frac{\mathbf{w}^H\mathbf{R}_n\mathbf{w}}{\mathbf{w}^H(\mathbf{R}-\mathbf{R}_n)\mathbf{w}}, \quad 1 \le n \le N, \tag{5}$$

where $\mathbf{R} = \mathbb{E}\left[\mathbf{r}\mathbf{r}^H\right]$, $\mathbf{R}_n = \mathbf{a}_n\mathbf{a}_n^H$, and $\mathbf{a}_n$ is the n^{th} column of $\mathbf{A}$. The solution of this optimization problem, known as the *generalized Rayleigh quotient*, is obtained by solving the generalized eigenvalue problem. Hence, $\mathbf{w}_n$ is the eigenvector corresponding to the maximum eigenvalue of $(\mathbf{R}-\mathbf{R}_n)^{-1}\mathbf{R}_n$ [18]. Alternatively, it can be shown that $\mathbf{w}_n$ can be calculated as a Wiener-Hopf beamformer given by [19]

$$\mathbf{w}_n = \mathbf{R}^{-1}\mathbf{a}_n. \tag{6}$$

Accordingly,

$$\mathbf{W} = \mathbf{R}^{-1}\mathbf{A}. \tag{7}$$

2) Noise Whitening Filter: In this section, we design a whitening filter for E-LGSD satellite receiver that whitens the noise by accounting for the spatial correlation amongst the LNBs. The covariance matrix of $\mathbf{n}'$ is given by

$$\mathbf{R}_{\mathrm{n}'\mathrm{n}'} = \sigma_{\mathrm{n}}^2\mathbf{F}^H\mathbf{G}\mathbf{F}, \tag{8}$$

where $\mathbf{G} \triangleq \mathbf{W}^H\mathbf{K}_{\mathrm{nn}}\mathbf{W}$. Note that for the considered overloaded scenario, $\mathbf{R}_{\mathrm{n}'\mathrm{n}'}$ is rank deficient. Thus, our goal is to find

$$\mathbf{F}_0 = \arg\min_{\mathbf{F}\in\mathbb{C}^{N\times N}} \|\mathbf{R}_{\mathrm{n}'\mathrm{n}'} - \mathbf{I}_N\|_F, \tag{9}$$

where $\mathbf{I}_N$ is the N-dimensional identity matrix. Since $\mathbf{K}_{\mathrm{nn}}$ is a covariance matrix, $\mathbf{G}$ is positive semi-definite. Hence, it can be written via the eigenvalue decomposition as $\mathbf{G} = \mathbf{U}\mathbf{L}\mathbf{U}^H$. Consequently, denoting the pseudo-inverse of $\mathbf{L}$ by $\mathbf{L}^\dagger$, it is easy to show that a solution of $\mathbf{F}_0$ can be determined as

$$\mathbf{F}_0 = \mathbf{U}\left(\mathbf{L}^\dagger\right)^{\frac{1}{2}}, \tag{10}$$

To reduce the complexity of E-LGSD, and obtain RC-LGSG, we exploit the structure of $\mathbf{F}_0$. Since the rank of $\mathbf{W}$ is M, $\mathbf{G}$, and consequently $\mathbf{L}$ are rank M. In other words, the last $(N-M)$ columns of $\mathbf{F}_0$ are zeros. Hence, the output of the noise whitening filter is independent of the last $(N-M)$ elements in the input vector. Consequently, these columns can be removed, resulting in a truncated noise whitening filter $\mathbf{T} \in \mathbb{C}^{N\times M}$. This implies that, after this truncation, the equivalent channel matrix at the input of the RC-LGSD detector (Fig. 3), and the whitened noise vector are

$$\begin{aligned}\mathbf{H} &\triangleq \mathbf{T}^H\mathbf{W}^H\mathbf{A} \quad \in \mathbb{C}^{M\times N},\\ \mathbf{z} &\triangleq \mathbf{T}^H\mathbf{W}^H\mathbf{n} \quad \in \mathbb{C}^{M},\end{aligned}$$

respectively. Note that $\mathbf{R}_{\mathrm{zz}} = \mathbb{E}\left[\mathbf{z}\mathbf{z}^H\right] = \sigma_{\mathrm{n}}^2\mathbf{I}_M$, i.e., the output of the preprocessor is uncorrelated. Finally, the input-output relation of the RC-LGS can be written as

$$\mathbf{y} = \mathbf{H}\mathbf{s} + \mathbf{z}. \tag{11}$$

B. Signal Detection

1) Joint Maximum-Likelihood (JML) Detection: Starting with the likelihood function

$$f\left(\mathbf{y}|\mathbf{H},\mathbf{s}\right) = \frac{1}{\left(2\pi\sigma_{\mathrm{n}}^2\right)^M}\exp\left(-\frac{\|\mathbf{y}-\mathbf{H}\mathbf{s}\|^2}{\sigma_{\mathrm{n}}^2}\right), \tag{12}$$

and noting that maximizing $f\left(\mathbf{y}|\mathbf{H},\mathbf{s}\right)$ is equivalent to minimizing $\|\mathbf{y}-\mathbf{H}\mathbf{s}\|^2$, the JML detector is given by

$$\hat{\mathbf{s}} = \arg\min_{\mathbf{s}\in\Omega^N} \|\mathbf{y}-\mathbf{H}\mathbf{s}\|^2. \tag{13}$$

Although the JML detector is an optimal detector, its complexity grows exponentially with the size of $\mathbf{s}$ and the modulation order. This motivates the design of suboptimal algorithms that reduce the detection complexity.

2) Reduced Complexity LGSD: Referring to Fig. 3, RC-LGSD consists of two entities: BLEs and a GLO. Although we use an approach similar to [10], the novelty of the proposed algorithm lies in its use of only M BLEs instead of N. This lower number of BLEs reduces the complexity of the detection algorithm with respect to [10]. This is made possible by the truncation introduced in Section III-A2. The conventional LGSD is briefly summarized below.

- Denote the index set by $\Gamma = \{1,2,...,N\} = \{\gamma_1,\gamma_2,...,\gamma_U\}$ such that $\gamma_i \cap \gamma_j = \phi, \forall i \neq j$.
- The index set γ_u is used to select a subset of the symbols in $\mathbf{s}$ and stack them in $\mathbf{s}_u \in \Omega^{|\gamma_u|}$, where $|\cdot|$ denotes the set cardinality, and to extract the corresponding row vectors of $\mathbf{H} \triangleq [H_{i,j}]$ so that $\mathbf{h}_u(m) = H_{u,m}\ \forall u \in \gamma_u,\ 1 \le m \le M$.
- The interference affecting the u^{th} group in the m^{th} BLE is cancelled by

$$y_m^{(u)} = y_m - \sum_{v=1,v\neq u}^{U} \mathbf{h}_v(m)\mathbf{s}_v, \tag{14}$$

  where $\mathbf{s}_v$ in (14) is drawn from the best signal vector obtained in the previous iteration by the LGSD detector[2].
- The search is then performed by calculating the mean-squared error (MSE) for all $\mathbf{s}_u \in \Omega^{|\gamma_u|}$ and $1 \le i \le K^{|\gamma_u|}$

$$e_i^{(u)} = \|y_m^{(u)} - \mathbf{h}_u(m)\mathbf{s}_u\|^2, \tag{15}$$

[2]This is the first vector in the GLO output list $\mathbf{S}$. However, in the first iteration, $\mathbf{S}$ is populated from Ω at random.

and the L candidate vectors of $\mathbf{s}_u$ with the lowest MSE are retained and de-mapped using γ_u to their branch candidate vector $\mathbf{s}_{\mathrm{br},m}^{(l)} \in \Omega^N$, $1 \leq \ell \leq L$.

- The branch candidate vector, $\mathbf{s}_{\mathrm{br},m}^{(l)}$, is sorted using

$$e_m^{(l)} = \|y_m - \mathbf{h}(m)\mathbf{s}_{\mathrm{br},m}^{(l)}\|^2, \tag{16}$$

to produce the branch list, $\mathbf{S}_{\mathrm{br},m} = \{\mathbf{s}_{\mathrm{br},m}^{(l)}\}$.

- The m^{th} BLE iterates over its own output I_{BLE} times, by feeding back the produced $\mathbf{S}_{\mathrm{br},m}$ to its input. Afterwards, all $\mathbf{S}_{\mathrm{br},m}$ are forwarded to the GLO.
- In the GLO, all the branch lists are concatenated into a major list of size $(N \times ML)$ that is again sorted by the MSE given by

$$e = \|\mathbf{y} - \mathbf{H}\mathbf{s}_{\mathrm{br},m}^{(l)}\|^2. \tag{17}$$

Only the first L candidate vectors are preserved in a list, $\mathbf{S}_{in}$, while the rest are discarded.

- The rows of the list $\mathbf{S}_{in}$ are partitioned according to the mapping γ_v, for $v = 1, \cdots, V$, resulting in V lists with dimensions $(|\gamma_v| \times L)$.
- The repeated vectors in these lists are dropped, resulting in V lists with size $(|\gamma_v| \times L_v)$, where $L_v \leq L$ is the number of the unique candidates in the v^{th} list.
- The GLO uses these lists to find the highly probable candidate list $\mathbf{S}$.
- Subsequently, The GLO output list is fed back to its input for a further iteration.
- After I_{GLO} GLO iterations, the final list is forwarded to the input of the BLE for a further global iteration. I_{GLB} iterations are performed globally by the LGSD.
- A sorted list containing the highest probable candidates is generated at the output of the GLO and only the first vector is demodulated.

More details about the LGSD algorithm can be found in [10].

IV. Complexity Analysis

In this section, we provide a complexity analysis of the RC-LGSD and compare it to the complexity of the JML detector. We also show the complexity reduction compared to the LGSD algorithm due to the truncation process presented in Section III-A2. As a measure of complexity, we use a criterion similar to that of [10], i.e., the number of real squaring operations required to obtain the Euclidean distance.

The computational complexity of the proposed RC-LGSD receiver can be calculated as

$$C(M) = 2I_{\mathrm{GLB}} \times \left(MI_{\mathrm{BLE}} \sum_{u=1}^{U} K^{|\gamma_u|} + I_{\mathrm{GLO}} \sum_{v=1}^{V} L_v |\gamma_v| K^{|\gamma_v|} + R \right), \tag{18}$$

where R is the number of the unique vectors in the major list at the input of the GLO. Note that, since L_v is the number of unique vectors in the v^{th} GLO sub-list, it varies from iteration to another, depending on GLO input list itself. Moreover, the first term in (18) corresponds to the computational complexity of the BLEs, while the remaining terms correspond to the complexity of GLO within the proposed detector.

A. The Complexity of RC-LGSD Compared to JML

In our investigations in Section V-B, we provide a complexity/performance trade-off for the RC-LGSD receiver using different iteration sets. The complexity in this trade-off is provided as a percentage of the JML complexity required for the same system dimensions. It is easy to show that the complexity of JML is given by $C_{\mathrm{JML}} = 2MK^N$. Therefore, the complxity of RC-LGSD for a receiver with M BLEs is

$$C_{\mathrm{RC}} = \frac{C(M)}{C_{\mathrm{JML}}} \times 100\% \tag{19}$$

B. Complexity of RC-LGSD Relative to LGSD and E-LGSD

In order to compare the complexity of the RC-LGSD with LGSD [10] and E-LGSD [15], we compute the complexity saving of RC-LGSD as a percentage of their complexity, both of which use N BLEs. This percentage is given by

$$C_{\mathrm{save}} = \frac{C(N) - C(M)}{C(N)} \times 100\%. \tag{20}$$

It can be shown that R is much smaller that the other terms in (18). Thus, (20) can be closely approximated by

$$C_{\mathrm{save}} \cong \frac{\left((N-M)I_{\mathrm{BLE}} \sum_{u=1}^{U} K^{|\gamma_u|}\right) \times 100\%}{NI_{\mathrm{BLE}} \sum_{u=1}^{U} K^{|\gamma_u|} + I_{\mathrm{GLO}} \sum_{v=1}^{V} L_v |\gamma_v| K^{|\gamma_v|}}.$$

Numerical investigations the computational complexity are presented in Section V-B.

V. Simulation Results and Discussion

A. Simulation Environment

In this section, we present the results of extensive simulations in practical settings, in terms of *uncoded* BER. We do that for the proposed receiver and compare it to schemes available in the literature. Since our objective is to detect the signal from the central satellite, and that this signal is the most prone to interference, we present the results of s_1 only.

1) Satellites Setup: We consider $N = 5$ GEO satellites stationed at orbital angles $0^\circ, 3^\circ, -2.8^\circ, 5.7^\circ$, and -5.9° as shown in Fig. 1.

2) Receiver Antenna Setup: We use $M = 3$ LNBs in conjunction with a 35-cm dish antenna that is directed towards the desired satellite s_1. The antenna radiation patterns are obtained using the satellite design software GRASP [20], which accepts the dimensions and the frequency as input parameters. GRASP is widely used in the satellite research and professional teams due to its accurate and realistic models. The resulting spatial correlation matrix for the considered setup is obtained using the patterns in Fig. 2 in conjunction with (2)

$$\mathbf{K}_{\mathrm{nn}} = \begin{pmatrix} 1.0 & 0.31 & 0.01 \\ 0.31 & 1.0 & 0.31 \\ 0.01 & 0.31 & 1.0 \end{pmatrix}. \tag{21}$$

3) Signals Format: The signals transmitted from the 5 satellites are assumed to be co-channel signals in the Ku-band. We focus on the high modulation orders, 8PSK and 16APSK, which are applied in the satellite broadcast systems, and conform to DVB-S2 and DVB-Sx standards. The constellation radius ratio of 16APSK is selected to be 2.85, in accordance

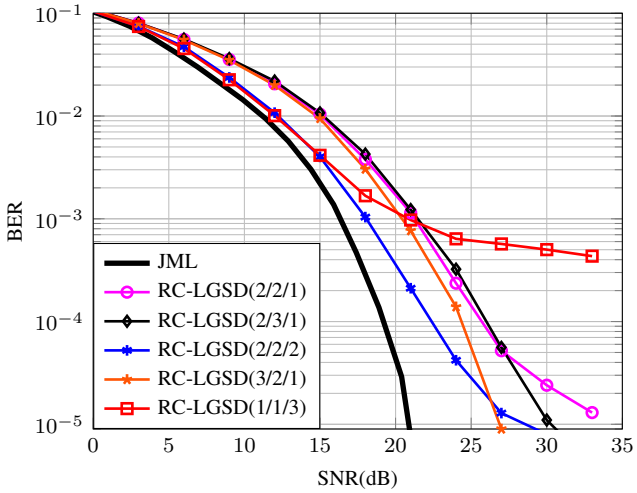

Fig. 4. Performance of 8PSK using different iteration sets.

with [8]. SNR is defined in terms of the average received signal power to noise power, i.e., $\text{SNR} = \|A\|_F^2/(\sigma_n^2 MN)$.

4) Algorithm Parameters: In this section, we use the notation X-LGSD($I_{\text{GLB}}/I_{\text{BLE}}/I_{\text{GLO}}$), where $I_{\text{GLB}}, I_{\text{BLE}}$ and I_{GLO} represent the number of iteration performed globally in the LGSD receiver, the number of iterations performed within the BLE, and the number of iterations performed within the GLO, respectively. For group partitioning, we use two group index sets, γ_1 and γ_2 of sizes 3 and 2, respectively. This grouping represents an acceptable trade-off between complexity and performance, since larger groups require searching over larger spaces, while by selecting smaller groups the advantages of joint processing diminish. A similar mapping is also utilized in the BLE and the GLO. Initially, the strongest 3 signals, s_1, s_2 and s_4 in Fig. 1 are mapped using γ_1, while s_3 and s_5 using γ_2. In the subsequent iterations, the group allocation is made at random to diversify the detection process in each iteration.

B. Complexity Reduction and Performance Trade-off

In this subsection, we investigate the effect of iteration numbers $I_{\text{GLB}}, I_{\text{BLE}}$, and I_{GLO} on the receiver performance and the incurred complexity. Subsequently, we select a suitable trade-off between performance and complexity and compare the proposed receiver to that of [10] and [15] for 8PSK and 16APSK modulations.

1) 8PSK transmission: Fig. 4 illustrates the performance of the receiver in terms of different number of iterations for 8PSK signals. In addition, Table I lists C_{save} and C_{RC} for different iteration values. The SNR values in Table I are the ones needed to reach a target BER value of 10^{-4}. Based on Fig. 4 and Table I we have the following observations:

- It can be inferred from Fig. 4 that increasing I_{GLB} enhances the performance of the receiver by eliminating the error floor at high SNR values. Moreover, for a larger I_{GLB}, the performance of the proposed RC-LGSD receiver approaches that of the JML. This can be seen considering the two scenarios RC-LGSD(3/2/1) and RC-LGSD(2/2/1), where there is 2 dB saving in the low-to-medium SNR and the error floor eliminated at higher SNR. This comes with an additional cost of 17% as indicated in Table I.

TABLE I
COMPLEXITY AND REQUIRED SNR OF DIFFERENT ITERATION SETS FOR 8PSK TRANSMISSION AT BER= 10^{-4}

$I_{\text{GLB}}/I_{\text{BLE}}/I_{\text{GLO}}$	SNR(dB)	C_{save} (%)	C_{RC} (%)
1/1/3	∞	2.7	42.4
2/1/1	26	7.1	30.6
2/1/2	22	3.9	57.7
2/1/3	20	2.7	84.7
2/2/1	25.5	12.1	34.1
2/2/2	22.5	7.1	61.2
2/2/3	20.5	5	88.2
2/3/1	26	15.7	37.6
2/3/2	23.5	9.8	64.7
2/3/3	20.4	7.1	91.8
3/1/1	24.5	7.1	45.9
3/1/2	21	3.9	86.5
3/2/1	24.3	12.1	51.2
3/3/1	24.6	15.7	56.4
JML	19.5	N/A	100

- Increasing I_{BLE} barely enhances the receiver performance at low-to-medium SNRs. However, in this setup, the larger BLE iterations result in a lower error floor at high SNR. This can be seen by comparing RC-LGSD(2/2/1) with RC-LGSD(2/3/1) in Fig. 4. This improvement in the overall performance of the system comes at the cost of overall receiver complexity, which is 3.5% higher for $I_{\text{BLE}} = 3$ as shown in Table I.
- Increasing I_{GLO}, enhances the receiver performance by shifting the BER plot to the left, closer to that of the JML. This outcome is illustrated in Fig. 4, where by increasing I_{GLO} from 1 to 2, for an additional complexity of 27%, RC-LGSD(2/2/2) results in a 3 dB performance gain compared to RC-LGSD(2/2/1).
- Although the computational complexities of RC-LGSD(1/1/3) and RC-LGSD(2/3/1) are 42.4% and 37.6% of that of the JML detector, respectively, RC-LGSD(2/3/1) exhibits a superior performance as illustrated in Fig. 4. Therefore, increasing the complexity of the proposed receiver does not necessarily reduce the required SNR to reach the target BER. As a result, the number of iterations in different blocks should be carefully selected.

Note that in some cases, the need for cheaper receivers surpasses the quality of the signal. Thus, Table I can be used to select a suitable trade-off between the affordable complexity and the associated performance.

2) 16APSK transmission: Fig. 5 and Table II highlight the results of our investigations with 16APSK signals. Table II lists multiple scenarios with different number of iterations, the associated complexity of each scenario, and the required SNR to achieve the target BER. We make the following observations:

- By increasing I_{GLB}, the error floor is significantly decreased at high SNRs, while for low-to-medium SNRs, the

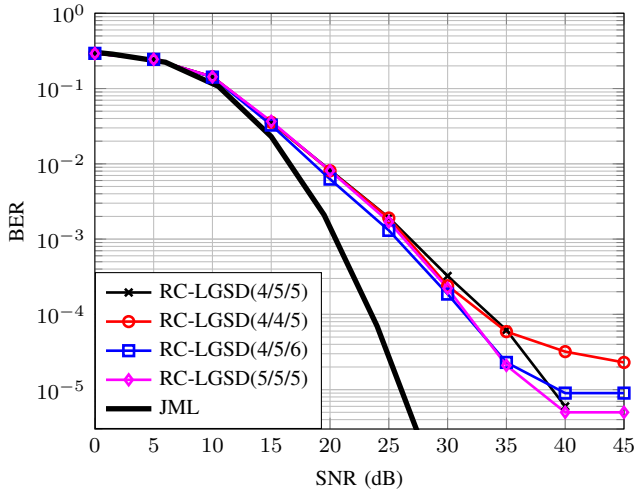

Fig. 5. Performance of 16APSK using different iteration sets.

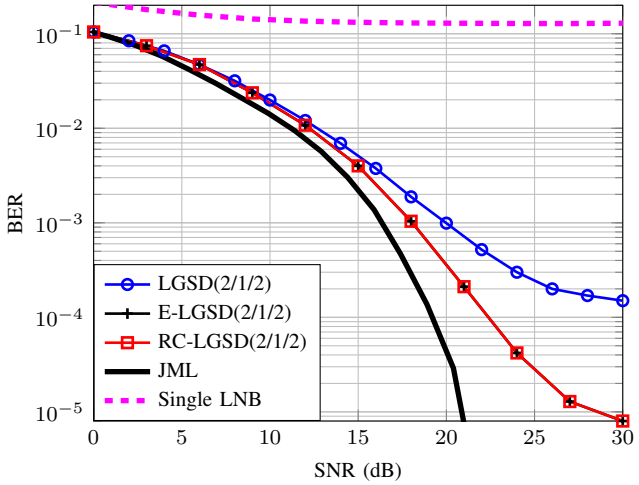

Fig. 6. Performance of 8PSK using different detectors.

BER performance is closer to that of the JML. For example, comparing RC-LGSD (4/5/5) with RC-LGSD(5/5/5), the overall performance of the system is enhanced by 1.2 dB, whenn reaching the target BER. However, this added performance gain comes at a complexity cost of 18%. This is similar to the effect observed when increasing I_{GLB} for 8PSK modulation in Section V-B1.

- On the other hand, removing one BLE iteration does not greatly degrades the performance of RC-LGSD, while greatly reducing its computational complexity. This can be observed when comparing the performance of RC-LGSD(4/5/5) with that of RC-LGSD(4/4/5) in Fig. 5, where the error floor at high SNR is slightly increased in the case of RC-LGSD(4/4/5).
- Our results indicate that increasing I_{GLO} can significantly enhance the BER performance of RC-LGSD, while also increasing the complexity. For example, RC-LGSD(4/5/6) is 13% more complex than RC-LGSD(4/5/5) but requires 1.5 dB less to reach the target BER. Higher I_{GLO} also reduces the error floor of the system performance.
- Comparing Tables I and II, it can be seen that in contrast to 8PSK, 16APSK is more sensitive to interference. This is reasonable since 16APSK is a denser two-ring modulation.

TABLE II
COMPLEXITY AND REQUIRED SNR OF DIFFERENT ITERATION SETS FOR 16APSK TRANSMISSION AT BER$= 10^{-4}$

$I_{\mathrm{GLB}}/I_{\mathrm{BLE}}/I_{\mathrm{GLO}}$	SNR(dB)	C_{save} (%)	C_{RC} (%)
4/4/4	35.5	7	56.6
4/4/5	33.5	5.8	69.1
4/4/6	31	5	81.6
4/5/4	35.5	8.4	58.2
4/5/5	33	7	70.7
4/5/6	31.5	6	83.3
4/6/4	35.5	9.6	59.8
4/6/5	33	8.1	72.4
4/6/6	32	7	84.9
5/4/4	33.5	7	70.7
5/4/5	31.8	5.8	86.4
5/5/4	33.8	8.4	72.8
5/5/5	31.8	7	88.4
5/6/4	31.8	9.6	74.8
6/4/4	32	7	84.9
6/5/4	31	8.4	87.3
JML	24	N/A	100

3) Selecting Iteration Set: The results in Figs. 4 and 5 show that I_{GLB} and I_{GLO} have a major impact on the system performance, while larger values of I_{BLE} increase the overall computational complexity of the receiver without significantly enhancing the BER. However, I_{BLE} dictate the BER floor of the receiver and a moderate value of I_{BLE} should be chosen.

For 8PSK signals, our results indicate that RC-LGSD(2/1/2) is a reasonable compromise between performance and complexity since its complexity is 57.7% of that of JML, while showing only a 3-dB poorer performance. Hence, it is used for comparison with existing schemes subsequently. On the other hand, for 16APSK signals, our results show that RC-LGSD(4/4/5) constitutes a reasonable trade-off between complexity and performance, since its complexity is 69.1% of that of JML, while showing a 9.5 dB poorer performance. Hence, RC-LGSD(4/4/5) is used for comparison with other schemes.

C. Performance Comparison

A comparison of the performance of RC-LGSD against that of the JML, conventional LGSD, and E-LGSD for 8PSK signals is presented in Fig. 6, which shows that compared to conventional LGSD(2/1/2), the BER performance of RC-LGSD(2/1/2) is closer to the lower-bound presented by the JML detector by a considerable margin. Moreover, the error floor for RC-LGSD(2/1/2) is significantly lower when compared to conventional LGSD(2/1/2). This can be attributed to the application of the proposed beamformer that takes into account the structure of the interference for satellite systems. On the other hand, although RC-LGSD(2/1/2) and E-LGSD(2/1/2) perform similarly, RC-LGSD is less complex with a 7.1% complexity saving as shown in Table I.

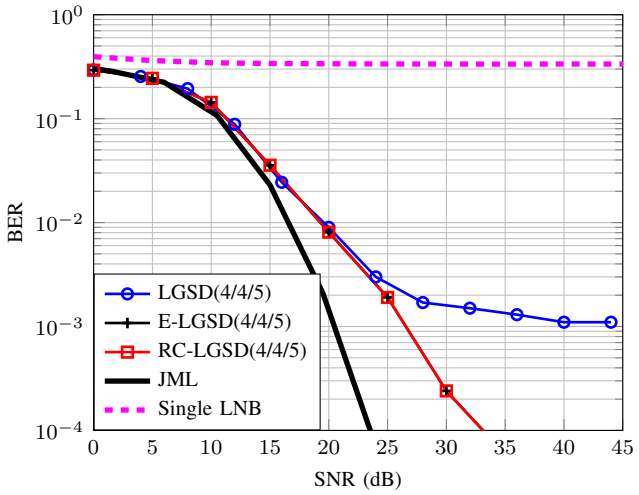

Fig. 7. Performance of 16APSK using different detectors.

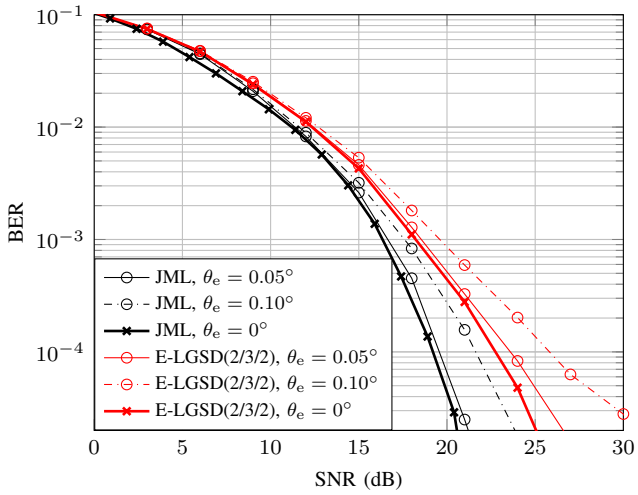

Fig. 8. Pointing error effect on 8PSK BER, for error angle $0.05°$ and $0.1°$.

Considering Fig. 7, the same comment can be made regarding the performance of RC-LGSD and E-LGSD in 16APSK signals. The complexity saving for the iteration set (4/4/5) for E-LGSD is 5.8% as compared to RC-LGSD. Moreover, when using the iteration set (4/4/5) for RC-LGSD and conventional LGSD, the error floor corresponding to RC-LGSD is significantly lower. This can be again attributed to the application of the proposed SINR-based beamforming approach in RC-LGSD compared to that of conventional LGSD.

Considering the cases in Figs. 6 and 7 where a single LNB is used in the presence of 3 satellites, the plots show very poor BER performance. This means that adding two more LNBs provides additional spatial diversity to the receiver and enhances the detection performance, despite the fact that the addition of more LNBs expands the field-of-view of the antenna and increases the system interference.

D. Pointing Error

In this section we investigate the sensitivity of the proposed receiver and the JML detector to pointing errors. Pointing error may occur due to various factors such as dish misalignment, satellite drifting, and wind deflection. Denote the pointing error by $\boldsymbol{\theta}' = [\theta'_n] \in \mathbb{R}^M$, where $\theta'_n \sim N(0, \sigma_e^2)$ such that the angle error range $\theta_e = 3\sigma_e$ [21]. Subsequently, the erroneous channel matrix can be written as a function of the satellite position and the error angle, that is $\mathbf{A}(\boldsymbol{\theta} + \boldsymbol{\theta}')$.

We assume that the procedure of *beam bracket peaking* is used during the antenna steering [22]. This procedure is capable of pointing the dish antenna so that the largest error angle is $\theta_e = 0.10°$ and the median error angle is $\theta_e = 0.05°$. These two values result in different pointing error distributions, and are investigated here separately. The performance of 8PSK RC-LGSD in the presence of these two pointing error distributions is presented in Fig. 8, where it can be seen that the performance of RC-LGSD deteriorates similar to that of the JML. More specifically, it is observed that a pointing error of $0.10°$ results in a $2.5 - 3.0$ dB performance loss when reaching the target BER. However, for a pointing error of $0.05°$, a $0.5 - 1.0$ dB loss is observed at the same BER value. It should be stressed, however, that although the effect of pointing errors on the performance of satellite systems can be mitigated, the investigation of such mitigation is beyond the scope of this paper. Nevertheless, the effect of pointing errors can be alleviated via channel estimation using the pilot structure of the DVB-S2 signals, or using accurate apparatus during the mechanical setup.

VI. Conclusions

In this paper, we presented an enhanced LGSD and reduced-complexity LGSD receivers that modify the linear preprocessor in the conventional LGSD receiver. The proposed receivers were applied to satellite broadcast systems in an overloaded setup. We used an SINR-based beamformer instead of the SNR-based approach applied in prior work. In addition, we designed a new noise whitening filter to suit the spatially correlated noise observed in the satellite broadcast systems. Furthermore, the computational complexity of the proposed receiver was further reduced via channel matrix truncation.

Focusing on the 8PSK and 16APSK modulations applied in satellite broadcast systems, extensive numerical simulations were executed to demonstrate the complexity/performance trade-off, and to compare the performance of the proposed receiver with those of existing algorithms. It was concluded that the allocation of a higher level complexity to different receiver blocks should be done with caution. It was also shown that compared to the conventional LGSD approach, the performance of the proposed receivers is closer to the optimal JML, while also reducing the computational complexity of the satellite receiver. In fact, for 8PSK and 16PSK we observe an SNR gain of 3 and 13 dB for a BER of 10^{-3}, respectively. Finally, the proposed receiver exhibits a similar behavior to that of the JML in the presence of pointing error.

References

[1] Satellite Industry Association, "State of the Satellite Industry Report," Sep 2015. [Online]. Available: http://www.sia.org/wp-content/uploads/2015/06/Mktg15-SSIR-2015-FINAL-Compressed.pdf

[2] B. Elbert, *Satellite Communication Applications Handbook*, 2nd ed. Artech House, Norwood, MA, USA, 2004.

[3] J. Grotz, J. Krause, and B. Ottersten, "Decision-directed interference cancellation applied to satellite broadcast reception," in *Proc. Vehicular Tech. Conf. Dallas, USA*, 2005.

[4] J. Grotz, B. Ottersten, and J. Krause, "Signal detection and synchronization for interference overloaded satellite broadcast reception," *IEEE Trans. Wireless Commun.*, vol. 9, no. 10, pp. 3052 –3063, Oct. 2010.

[5] Z. Abu-Shaban, H. Mehrpouyan, J. Grotz, and B. Ottersten, "Overloaded satellite receiver using SIC with hybrid beamforming and ML detection," in *Proc. of 14th Workshop on Signal Processing Advances in Wirelss Commun. (SPAWC), Darmstadt, Germany*, June 2012, pp. 421 –425.

[6] B. Beidas, H. El Gamal, and S. Kay, "Iterative interference cancellation for high spectral efficiency satellite comm." *IEEE Trans. Commun.*, vol. 50, no. 1, pp. 31 –36, Jan. 2002.

[7] K. Schwarzenbarth, J. Grotz, and B. Ottersten, "MMSE based interference processing for satellite broadcast reception," in *Proc. Vehicular Tech. Conf., Dublin, Ireland*, Apr. 2007, pp. 1345 –1349.

[8] The European Telecom. Standards Institute (ETSI), "EN 302 307: Digital Video Broadcasting; second generation framing structure, channel coding and modulation systems for broadcast, interactive services, news gathering and broadband satellite applications." *ETSI*, Feb. 2005.

[9] S. Bayram, J. Hicks, R. Boyle, and J. Reed, "Joint maximum likelihood approach in overloaded array processing," in *Proc. Vehicular Tech. Conf. Tokyo, Japan*, vol. 1, 2000, pp. 394–400.

[10] M. Krause, D. Taylor, and P. Martin, "List-based group-wise symbol detection for multiple signal comm." *IEEE Trans. Wireless Commun.*, vol. 10, no. 5, pp. 1636 –1644, May 2011.

[11] J. Hicks, S. Bayram, W. Tranter, R. Boyle, and J. Reed, "Overloaded array processing with spatially reduced search joint detection," *IEEE J. Sel. Areas Commun.*, vol. 19, no. 8, pp. 1584 –1593, Aug 2001.

[12] A. Kapur and M. Varanasi, "Multiuser detection for overloaded CDMA systems," *IEEE Trans. Inf. Theory*, vol. 49, no. 7, pp. 1728 – 1742, Jul. 2003.

[13] G. Colman and T. Willink, "Overloaded array processing using genetic algorithms with soft-biased initialization," *IEEE Trans. Veh. Technol.*, vol. 57, no. 4, pp. 2123 –2131, July 2008.

[14] S. Grant and J. Cavers, "Performance enhancement through joint detection of cochannel signals using diversity arrays," *IEEE Transactions on Comm.*, vol. 46, no. 8, pp. 1038–1049, Aug. 1998.

[15] Z. Abu-Shaban, B. Shankar, H. Mehrpouyan, and B. Ottersten, "Enhanced list-based group-wise overloaded receiver with application to satellite reception," in *2014 IEEE Int. Conf. on Comm. (ICC)*, June 2014, pp. 5616–5621.

[16] A. K. Maini and V. Agrawal, *Satellite Technology: Principles and Applications*, 2nd ed. John Wiley & Sons, Chichester, UK, Oct. 2010.

[17] H. T. Hui, "Influence of antenna characteristics on MIMO systems with compact monopole arrays," *IEEE Antennas and Wireless Propagation Letters*, vol. 8, pp. 133–136, 2009.

[18] T. De Bie, N. Cristianini, and R. Rosipal, "Eigenproblems in pattern recognition," in *Handbook of Geometric Computing: Applications in Pattern Recognition, Computer Vision, Neural computing, and Robotics*. E. B. Corrochano, ed. Berlin Heidelberg, Germany: Springer, 2005, pp. 128–132.

[19] H. L. Van Trees, *Adaptive Beamformers*. John Wiley & Sons, Inc. New York, USA, 2002, pp. 710–916.

[20] Ticra, "GRASP® student edition 10.0.1," 2013. [Online]. Available: http://www.ticra.com/

[21] R. O. Hughes, "Monte Carlo analysis of satellite beam pointing errors," *AIAA Journal of Guidance, Control, and Dynamics*, vol. 15, pp. 35–39, 1992.

[22] R. Brooker and D. Vorderbrueggen, "Antenna pointing accuracy impact on geostationary satellite link quality and interference," in *Proc. of the 23rd AIAA Int. Comm. Satellite Systems and 11th Ka and Broadband Comm. Joint Conf., Rome, Italy*, October 2005.